

https://doi.org/10.1070/QEL16998

Optical pumping of ultracold thulium atoms to a lower level of the clock transition and study of their depolarisation

E.S. Fedorova, D.O. Tregubov, A.A. Golovizin, G.A. Vishnyakova, D.A. Mishin, D.I. Provorchenko, K.Yu. Khabarova, V.N. Sorokin, N.N. Kolachevsky

Abstract. **The atomic energy levels corresponding to states with the zero projection of the total angular momentum have a weak sensitivity to certain sources of shifts and, therefore, are widely used in precision spectroscopy. The optical pumping of ultracold thulium atoms to the ground state level with the zero projection of the total angular momentum is described. The population dynamics of this state due to magnetic dipole–dipole interaction in an external magnetic field is studied.**

Keywords: *optical pumping, optical clock, clock transition, depolarisation, ultracold atoms, thulium.*

1. Introduction

Atom pumping to specific levels including those with a certain projection of the total angular momentum m_F is an actual problem in precision spectroscopy [1], physics of ultracold atoms [2], and quantum informatics and sensors [3,4]. In optical frequency standards, the interrogation method for a clock transition depends on the total atomic angular momentum F. Thus, in the case of integer F, the transition between central magnetic components with $m_F = 0$ and $m'_F = 0$ is used [5,6]; and for half-integer values, the transitions from maximally polarised magnetic sublevels are alternately interrogated [7,8]. A clock transition in thulium-based optical clocks being developed is the inner-shell transition ($J = 7/2$, $F = 4$, $m_F = 0$) → ($J' = 5/2$, $F' = 3$, $m'_F = 0$) between fine-structure sublevels of the ground state at $\lambda = 1.14$ μm [9]. Here, J is the total electronic angular momentum of the atom. For the states with $m_F = 0$, the linear Zeeman shift is zero; correspondingly, the shift of the clock transition, which is quadratic in the magnetic field intensity is small. In addition, the shift of the level due to magnetic dipole–dipole interaction between atoms is also zero. For the thulium atom it is especially important because it has a large dipole moment in the ground state $\mu = 4\mu_B$ (μ_B is the Bohr magneton).

Thus, the necessary stage in designing optical clocks on thulium atoms is pumping atoms to the central magnetic sublevel of the ground state with $m_F = 0$. The problem can be solved in various ways [10–12]. One of those is the optical pumping by a linearly polarised radiation, which excites the transition between the hyperfine sublevels having equal values of the total angular momentum ($F = F'$). For $\Delta F = F' - F = 0$, the transition $|m_F = 0\rangle \rightarrow |m'_F = 0\rangle$ is forbidden. Hence, the sublevel $m_F = 0$ is 'dark' for a linearly polarised radiation, which increases its population due to atom spontaneous decay from the states with $m'_F = \pm 1$. The thulium nuclear spin is $I = 1/2$; consequently, all its energy levels split into two hyperfine components. Thus, the two kinds of transitions can be used for optical pumping by linearly polarised radiation: 1) with a change in the total electronic angular momentum J ($|J = 7/2\rangle \rightarrow |J' = J + 1 = 9/2\rangle$) (Fig. 1a) and 2) without such a change ($|J = 7/2\rangle \rightarrow |J' = J = 7/2\rangle$) (Fig. 1b); in both cases, we have $F = F' = 4$. The hyperfine level structure in the first case makes it possible to realise laser cooling on the transition $|J = 7/2, F = 4\rangle \rightarrow |J' = 9/2, F' = 5\rangle$, which is used in our experiments for forming a magneto-optical trap (MOT). Correspondingly, for the optical pumping we can employ the same laser system with the emission wavelength of 530.7 nm as that for laser cooling. A drawback of this method is that in the result of spontaneous decay, the atom from the state $|J' = 9/2, F' = 4\rangle$ transits to the state $|J = 7/2, F = 3\rangle$ (the corresponding transition probability ratio is $w_{F'=4\rightarrow F=3}/w_{F'=4\rightarrow F=4} = 35$); that is, the transition $|J = 7/2, F = 4\rangle \rightarrow |J' = 9/2, F' = 4\rangle$ is not cyclic. In the second case, the transition $|J = 7/2, F = 4\rangle \rightarrow |J' = 7/2, F' = 4\rangle$ is almost cyclic (the transition probability ratio is $w_{F'=4\rightarrow F=3}/w_{F'=4\rightarrow F=4} = 1/35$); however, the optical pumping in this case requires an additional laser system, for example, with a wavelength of 418.8 nm.

We have realised efficient optical pumping of thulium atoms to the magnetic sublevel with $m_F = 0$ of the ground state by using the transition $|J = 7/2, F = 4\rangle \rightarrow |J' = 9/2, F' = 4\rangle$ at $\lambda = 530.7$ nm with the natural linewidth $\gamma = 350$ kHz, which is also used for secondary cooling of thulium atoms (case 1). Atom escape from the pumping cycle was prevented by using the repumping radiation, which simultaneously excited the hyperfine component $|J = 7/2, F = 3\rangle \rightarrow |J' = 9/2, F' = 4\rangle$. The optimal radiation parameters of optical pumping were found numerically and then experimentally. In addition, the time dependence of thulium central magnetic sublevel population in a one-dimensional optical lattice was studied and the depolarisation rate due to dipole–dipole interaction was measured.

2. Optical pumping, numerical simulation

The diagram of the energy levels involved in the optical pumping is shown in Fig. 1a. For shortness, we use the fol-

E.S. Fedorova, K.Yu. Khabarova, V.N. Sorokin, N.N. Kolachevsky P.N. Lebedev Physical Institute, Russian Academy of Sciences, Leninsky prosp. 53, 119991 Moscow, Russia; Russian Quantum Centre, ul. Novaya 100, Skolkovo, 143025 Moscow, Russia; e-mail: kalganova.elena@gmail.com;
D.O. Tregubov, A.A. Golovizin, G.A. Vishnyakova, D.A. Mishin, D.I. Provorchenko P.N. Lebedev Physical Institute, Russian Academy of Sciences, Leninsky prosp. 53, 119991 Moscow, Russia;

Received 12 March 2019; revision received 18 March 2019
Kvantovaya Elektronika **49** (5) 418–423 (2019)
Translated by N.A. Raspopov

lowing designations for the states considered: $|1\rangle \equiv |J = 7/2, F = 4\rangle$; $|2\rangle \equiv |J = 7/2, F = 3\rangle$; $|3\rangle \equiv |J' = 9/2, F' = 4\rangle$. The level $|J' = 9/2, F' = 5\rangle$ is used only in the cooling cycle and does not participate in the optical pumping. The system under consideration comprises 25 magnetic sublevels of states $|1\rangle$, $|2\rangle$, and $|3\rangle$ interacting with two linearly polarised light fields that couple levels $|1\rangle \rightarrow |2\rangle$ (the pump radiation) and $|2\rangle \rightarrow |3\rangle$ (repumping radiation) in an external magnetic field. Hereinafter, the direction of the external magnetic field determines a quantisation axis, the polarisations of the pumping and repumping electric fields are aligned with the magnetic field in order to excite the transitions without a change in the projection of the total angular momentum m_F. The population of the central sublevel was determined by solving Liouville equation for a density matrix. Calculations were performed using QuTiP [13].

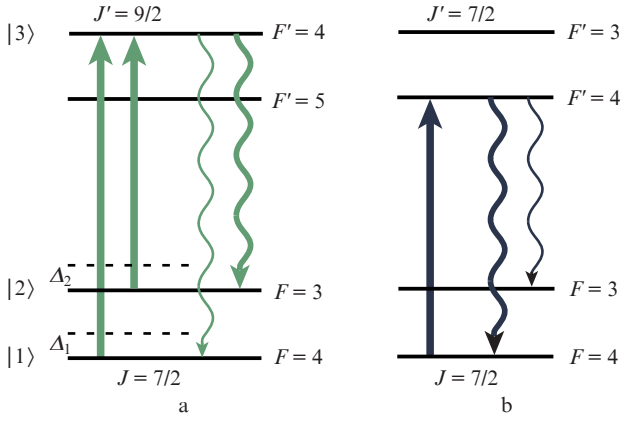

Figure 1. Two kinds of transitions in the thulium atom, which can be used for optical pumping to the magnetic sublevel with $m_F = 0$ of the ground state: (a) $|J = 7/2, F = 4\rangle \rightarrow |J' = 9/2, F' = 4\rangle$ and (b) $|J = 7/2, F = 4\rangle \rightarrow |J' = 7/2, F' = 4\rangle$, and $|1\rangle, |2\rangle, |3\rangle$ are the levels considered in modelling the optical pumping with the transition at a wavelength of 530.7 nm. Straight lines correspond to the transitions that should to be excited in the optical pumping, wavy lines correspond to spontaneous decay channels.

In the rotating wave approximation, the Hamiltonian of the system considered has the form [14]:

$$H = H_{\mathrm{A}} + V_{\mathrm{AL}}, \tag{1}$$

$$H_{\mathrm{A}} = \sum_{q \in \{1,2,3\}} \sum_{m_q} (h\Delta_q + m_q \mu_{\mathrm{B}} g_q B_0) |q, m_q\rangle\langle q, m_q|,$$

$$V_{\mathrm{AL}} = \sum_{q \in \{1,2\}} \sum_{m_q} \sum_{m_3} \frac{h}{2} \Omega(3, m_3; q, m_q) \{|3, m_3\rangle\langle q, m_q| + |q, m_q\rangle\langle 3, m_3|\}.$$

Here, B_0 is the external magnetic field induction; h is the Planck constant; Δ_q is the radiation frequency detuning from the frequency of unperturbed transition (in what follows, simply detuning); the summand H_{A} describes atom in a magnetic field, and V_{AL} accounts for atom interaction with the pump and repumping radiations; the energy of the level $|3\rangle$ is taken zero; $\Delta_3 = 0$; m_q is the projection of the total angular momentum of the level $|q\rangle$; g_q is the Lande g-factor for the level $|q\rangle$; $q \in \{1, 2, 3\}$ ($g_1 = 1$, $g_2 = 1.28$, $g_3 = 1.24$); and $\Omega(3, m_3; 1, m_1)$ and $\Omega(3, m_3; 2, m_2)$ are the Raby frequencies for the pump and repumping radiations, respectively, which are given by the expression [14]

$$\Omega(3, m_3; q, m_q) = (-1)^{m_q + F_q + 1} \times \gamma \sqrt{(2F_q + 1)(2F_3 + 1)(2J_q + 1)} \times \begin{pmatrix} F_q & 1 & F_3 \\ -m_q & 0 & m_3 \end{pmatrix} \begin{Bmatrix} J_3 & J_q & 1 \\ F_q & F_3 & I \end{Bmatrix} \sqrt{\frac{S_q}{2}}, \quad q = 1, 2. \tag{2}$$

Here, γ is the natural linewidth of the transition; and S_1 and S_2 are the saturation parameters for the pump and repumping radiations, respectively. The evolution of population η of the central magnetic sublevel of the ground state is shown in Fig. 2 at the pump parameters corresponding to the experiment.

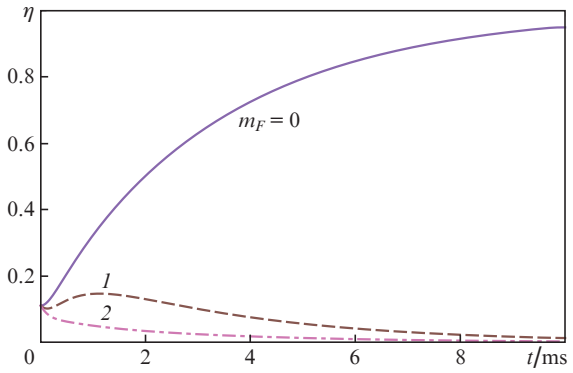

Figure 2. Populations of the magnetic sublevels $m_F = 0, 1$, and 2 of the ground state vs. the duration of optical pumping (numerical solution). The parameters of the pump and repumping radiations are: $S_1 = 4.4$, $S_2 = 4$, $\Delta_1 = -0.3\gamma = -0.1$ MHz, and $\Delta_2 = -2.3\gamma = -0.8$ MHz, $B_0 = 0.45$ G.

In calculations, we maximised the population of the central magnetic sublevel with $m_F = 0$ attained in the pump cycle of duration $\tau_{\mathrm{pump}} = 5$ ms; for this purpose, the values of the external magnetic field, intensity and detuning of the pump and repumping radiations were varied. Figure 3 presents some results obtained, namely, dependences of the population of the central magnetic sublevel with $m_F = 0$ under the optical pumping of duration 5 ms on the value of the external magnetic field B_0 and pump radiation detuning Δ_1, on the intensities of the pump and repumping radiations (S_1 and S_2), and on the detunings of the pump and repumping radiations (Δ_1 and Δ_2). The calculations show that the optical pump rate monotonously increases with intensities of the pump and repumping radiations (within the range of experimental conditions available). Therefore, in experiments, the maximal intensities of the pump and repumping radiations were taken ($S_1 = 4.4$, $S_2 = 4$). In Fig. 3, one can see that at certain relation between the magnetic field and detunings, the system exhibits coherent population trapping (CPT), which reveals in a reduced population η; hence, the magnetic field and detunings of the pump and repumping radiation should be chosen consistently. The magnetic field induction B_0 should be sufficiently large to split the projection of the total angular momentum for all the levels considered; the value of Zeeman splitting should exceed the natural width of the transition line $\Delta E/h = \mu_{\mathrm{B}} g_3 B_0/h > \gamma$,

which in our case holds at $B_0 > 0.2$ G. In the experiment, the magnetic field induction B_0 was constant and equal to 0.45 G. The corresponding optimal detunings, at which the population $\eta = 1$ is reached during the pump cycle of duration 5 ms, are $\Delta_1 = \Delta_2 = 0$.

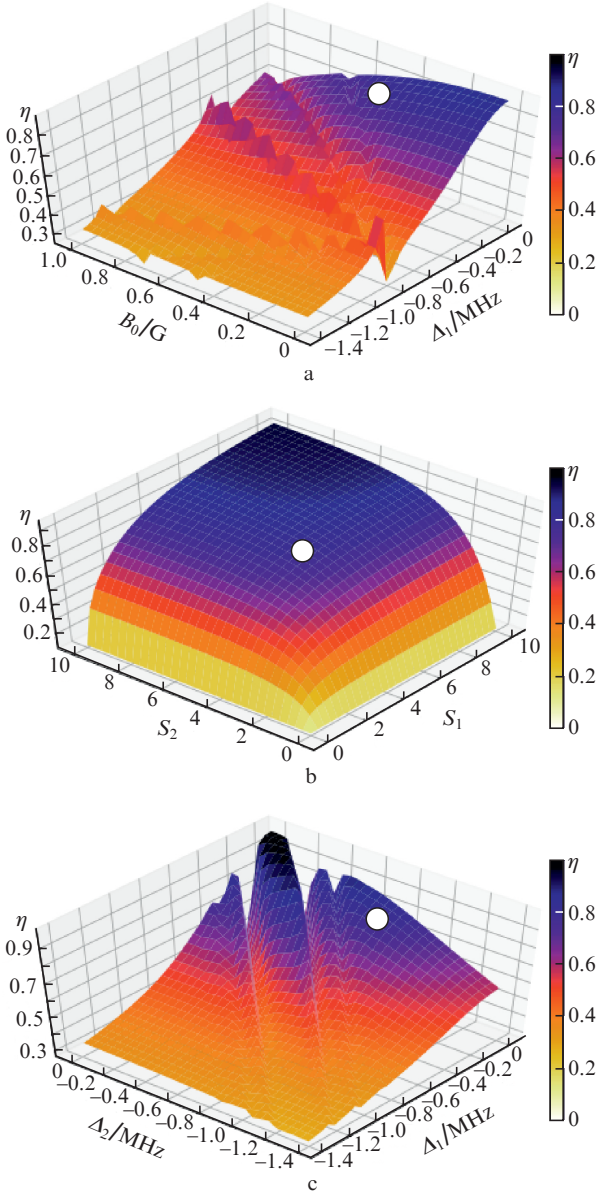

Figure 3. (Colour online) Populations η of the central magnetic sublevel of the ground state after optical pumping with a duration of 5 ms (numerical solution): (a) $S_1 = 4.4$, $S_2 = 4$, $\Delta_2 = -2.3\gamma = -0.8$ MHz; (b) $\Delta_1 = -0.3\gamma = -0.1$ MHz, $\Delta_2 = -2.3\gamma = -0.8$ MHz, $B_0 = 0.45$ G; and (c) $S_1 = 4.4$, $S_2 = 4$, $B_0 = 0.45$ G. In each plot, the points are marked with the coordinates, respectively, $\eta = 0.8$, $B_0 = 0.45$ G, $\Delta_1 = -0.3\gamma = -0.1$ MHz; $\eta = 0.8$, $S_1 = 4.4$, $S_2 = 4$; $\eta = 0.8$, $\Delta_2 = -2.3\gamma = -0.8$ MHz, $\Delta_1 = -0.3\gamma = -0.1$ MHz, which correspond to the experimental data (Fig. 5).

3. Optical pumping. Experiment

Optical pumping of thulium atoms in an optical lattice to the central magnetic sublevel of the ground state was experimentally realised. A schematic of the experimental setup is shown in Fig. 4. A sequence of used laser pulses is also presented in the figure. Preliminarily, atoms were cooled in a magneto-optical trap and were captured to a vertical optical lattice at a wavelength of 813.3 nm. Cooling processes in MOT and atom reload into the lattice are described in [15, 16]. Magnetic sublevels were split by applying the horizontally oriented bias magnetic field $B_0 = 0.45$ G just after MOT switches off. In a time delay of 20 ms after switching on the magnetic field, the pump and repumping radiations switched on for a time interval of τ_{pump}. The delay after switching on the magnetic field is needed for all transient processes to finish. The pump and repumping beams spatially coincide in the vacuum chamber, polarisations of both the beams were linear, and the polarisation vectors were parallel to the magnetic field vector. Thus, the experiment realised the system of the energy levels and light fields coupling them described by Hamiltonian (1), which was considered in the numerical simulation. In the present work, direct and back-reflected beams were superimposed, forming one-dimensional optical molasses; this partially compensated for atom heating by the pump and repumping radiations.

The efficiency of optical pumping was determined by spectroscopy of the clock transition at $\lambda = 1.14$ μm, described in [17]. After a pump cycle, the transition between central mag-

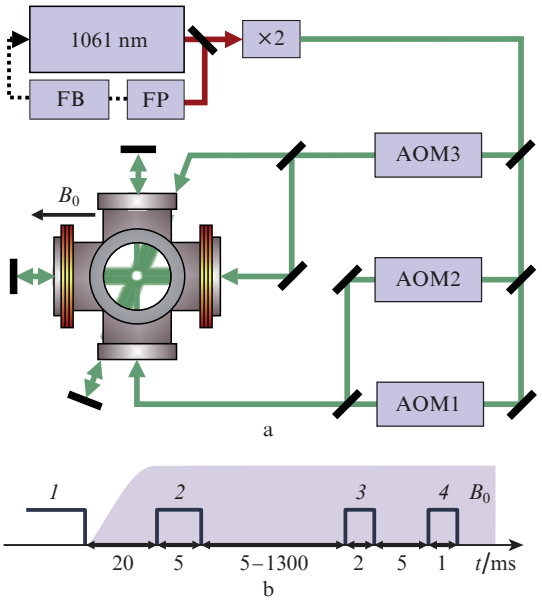

Figure 4. (a) Schematic of the experimental setup. The frequency of a semiconductor laser radiation at $\lambda = 1061$ nm is stabilised relative to the external high-Q Fabry–Perot ULF-cavity (FP) by a feedback (FB) system and is doubled ($\lambda = 530.7$ nm). Then the double frequency is shifted by acousto-optical modulators AOM1 (for the optical pumping), AOM2 (to return atoms to the pump cycle – repumping radiation), and AOM3 (for laser cooling). The third beam for laser cooling, which is normal to the image plane, is not shown. A uniform magnetic field B_0 is directed along the electric field vector of the linearly polarised pump radiation. (b) Scheme of a laser pulse sequence. After finishing the cooling (*1*), atoms are partially captured in the optical lattice. For optical pumping, the uniform magnetic field B_0 is switched on. After the field attains a stationary value, the optical pumping continues for 5 ms (*2*). Then, the clock transition $|m_F = 0\rangle \rightarrow |m'_F = 0\rangle$ is excited by a π-pulse of linearly polarised radiation at wavelength $\lambda = 1.14$ μm (*3*), and the number of atoms remaining in the ground state is determined by the luminescence signal under the action of the resonance probe radiation at $\lambda = 410.6$ nm (*4*). In the experiment on measuring the rate of depolarisation, the time delay between the pulses of optical pumping and clock transition excitation was varied.

netic components of the ground and upper clock levels was excited by a pulse of linearly polarised radiation of duration 2 ms with the intensity corresponding to a π-pulse at zero detuning. A frequency of the clock transition was scanned and the probability of exciting the state $|m'_F = 0\rangle$ was measured by the level of luminescence of unexcited atoms. Note that the Raby frequencies and, correspondingly, durations of π-pulses differ for atoms in different vibrational states of the optical lattice potential, which limits the maximal excitation efficiency. In the result, the maximal excitation probability yields the lower bound for the relative population of the central magnetic sublevel $|m'_F = 0\rangle$. For obtaining the maximal population, the duration of the pump pulse, radiation intensities, and detunings were varied. For initial approximation, the results of numerical simulation were used $B_0 = 0.45$ G, $\Delta_1 = \Delta_2 = 0$, $S_1 = 4.4$, and $S_2 = 4$. The following optimal parameters were determined experimentally: $\tau_{\text{pump}} = 5$ ms, $S_1 = 4.4$, $S_2 = 4$, $\Delta_1 = -0.1$ MHz, and $\Delta_2 = -0.8$ MHz. In these conditions, the relative population was $\eta = 0.79(2)$ (Fig. 5); part of atoms remaining trapped in the optical lattice after the pump cycle was 60%. The substantial losses of atoms from the lattice are related to atom heating due to multiple scattering of repumping radiation photons. The distinction between calculated and experimentally determined parameters of the pump and repumping radiations probably relates to the fact that the modelling neglected atom heating and differential scalar and tensor polarisabilities. In addition, nonlinearity of the pump radiation polarisation or misalignement of the polarisation from the axis defined by the magnetic field may lead to excitation of atoms on the central sublevel of the ground state and reduce the overall degree of polarisation. However, experimental data sufficiently well agree with the calculation results, which give a good initial approximation for further experimental search for optimal parameters of the optical pumping.

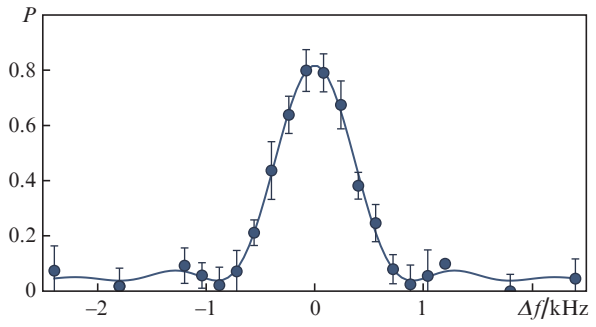

Figure 5. Experimentally measured probability P of populating the sublevel $|m'_F = 0\rangle$ by a 2-ms π-pulse vs. frequency detuning Δf of the clock transition laser (λ =1.14 μm, points). The curve is approximation of experimental data by the function $\text{sinc}^2(\pi\tau\Delta f)$.

The method of optical pumping described above is relatively simple in implementation, because it requires no additional laser sources: the radiation frequencies needed are obtained by using a cooling laser and acousto-optical modulators. Nevertheless, this approach results in heating the ensemble and atom losses from the trap because atoms from the excited state mainly decay to sublevel $|J = 7/2, F = 3\rangle$ of the ground state from where those should be returned to the pump cycle by additional radiation. It can be obviated by using for pumping a transition, which involves levels with equal values of the total electronic angular momentum $|J = 7/2\rangle \rightarrow |J' = J = 7/2\rangle$, for example, the transition at $\lambda = 418.8$ nm with a natural linewidth $\gamma = 10.2$ MHz. The wavelength of this transition is convenient from the viewpoint of availability of laser radiation sources; its linewidth is sufficient for realising fast optical pumping.

4. Depolarisation

In an external magnetic field, the central magnetic sublevel of the ground state $m_F = 0$ is not a lowest-energy state, and the depolarisation process occurs in a polarised atomic ensemble: spin flips due to interatomic magnetic dipole–dipole interaction. The process may limit the duration of clock transition interrogation (which affects the spectral width of the line) and, as shown below, result in atom losses from the trap. Earlier, we calculated the depolarisation rates for thulium atoms in a two-dimensional optical lattice [9] without magnetic field. The calculations show that the population of the central magnetic sublevel should fall by 30% in a time interval of 10 ms if the occupation number of cells of the two-dimensional lattice is close to unity. The calculations were performed for a fixed distance between antinodes of the two-dimensional optical lattice. In a one-dimensional optical lattice, where atomic motion is limited in one direction, the average distance between atoms is substantially greater. We may also expect that in a magnetic field the rate of depolarisation will reduce.

In order to describe the rates of depolarisation due to magnetic dipole–dipole interaction in the presence of an external uniform magnetic field B_0, consider two interacting atoms possessing magnetic dipole momenta $\boldsymbol{\mu}_1$ and $\boldsymbol{\mu}_2$, which mutual position is given by a vector $\boldsymbol{r}$. The Hamiltonian of this system consists of two parts: $H = H_Z + V_{\text{DDI}}$, where H_Z is Zeeman interaction of atom with the external magnetic field, and

$$V_{\text{DDI}} = \frac{1}{4\pi r^3}[\boldsymbol{\mu}_1\boldsymbol{\mu}_2 - 3(\boldsymbol{\mu}_1\boldsymbol{r})(\boldsymbol{\mu}_2\boldsymbol{r})]$$

$$= \frac{\mu_1\mu_2}{4\pi r^3}[T_0 + T'_0 + T_1 + T_{-1} + T_2 + T_{-2}]$$

is the dipole–dipole interaction [18]. Here, the summand T_0 describes the elastic dipole–dipole interaction, for which the projection of the total angular momentum of each atom remains unchanged; T'_0 describes the simultaneous change of the projections of total angular momenta of two atoms by plus or minus one, in which their sum remains constant as well as the total internal energy of the system; and T_1, T_{-1}, T_2, and T_{-2} correspond to the relaxation processes in which the internal energy of Zeeman interaction transfers to a kinetic energy and vice versa due to a change of the sum of projections of total angular momenta.

The energy corresponding to the change by unity of the projection of the totoal angular momentum for one of the atoms is equal to the value of Zeeman splitting $\Delta E = \mu_B g B$. In the considered experiment, a typical magnetic field value is 0.45 G, which corresponds to the energy $\Delta E/k_B = 30$ μK. A depth of the optical lattice potential U/k_B in our case is at most 20 μK, that is, the change in the sum of projections of the totoal angular momenta due to the reduction of the kinetic energy is suppressed because only a small part of atoms in the dipole trap has a sufficient energy. In turn, relaxation accom-

panied by an increase in the kinetic energy leads to atom loss from the dipole trap. Thus, relaxation processes do not change the relative population of magnetic sublevels, but affect only the total number of atoms in the trap. Hence, in the dependence of the relative population of central magnetic sublevel on time we may limit our consideration to the first two summands in the expression for V_{DDI}. In this case, depolarisation is described by the following Schrödinger equations:

$$i\hbar\frac{\partial\psi}{\partial t} = [H_{\mathrm{Z}} + \xi(r)\,T_0 + \xi(r)\,T_0']\psi. \qquad (3)$$

Here,

$$H_{\mathrm{Z}} = g\mu_{\mathrm{B}}BS_{1z} + g\mu_{\mathrm{B}}BS_{2z};$$

$$\xi(r) = -\frac{\mu_1\mu_2}{4\pi r^3};$$

$$T_0 = (3\cos^2\theta - 1)S_{1z}S_{2z};$$

$$T_0' = 1/4(3\cos^2\theta - 1)(S_{1+}S_{2-} + S_{1-}S_{2+});$$

S_{iz}, S_{i+}, S_{i-} are the operator of the projection of the total angular momentum, raising and annihilation operators affecting the total angular momentum of ith atom ($i = 1, 2$); and θ is the polar angle, which defines the direction of $\boldsymbol{r}$ (see inset in Fig. 6). For the initial system state, we take $|m_1 = 0, m_2 = 0\rangle$ where both atoms have zero total angular momentum projections to the quantisation axis. Numerical solutions for Eqn (3) are presented in Fig 6 for several distances between dipoles.

The depolarisation rate in the optical lattice configuration employed was experimentally measured. For this purpose, atoms in the lattice were pumped to the central magnetic sublevel. Then, the excitation probability for the state $|m_F' = 0\rangle$ was measured in a time interval $\tau_{\mathrm{delay}} = 5 - 1300$ ms (Fig. 4b). Measurement results are shown in Fig. 6. By approximating experimental data with numerical simulation, we found the average distance between atoms $r = 1.24(6)$ μm.

One can see from Fig. 6 that the population of the magnetic sublevel with $m_F = 0$ changes by less than 20% in a time interval of 1 s. At the interrogation period $\tau = 1$ s, the transform-limited line width does not exceed 1 Hz, which is less than the natural linewidth of the clock transition. Hence, in the optical lattice geometry described, at the atom concentration $n \sim 10^{11}$ cm^3, depolarisation due to magnetic dipole–dipole interaction actually does not limit the interrogation time and width of the clock transition resonance.

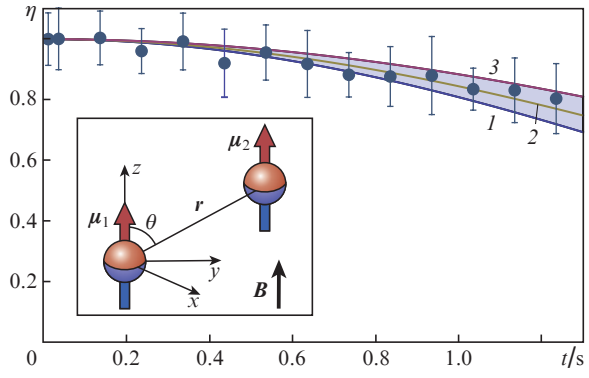

Figure 6. Dynamics of the relative population of the central magnetic sublevel in an ensemble of thulium atoms in a one-dimensional optical lattice due to magnetic dipole–dipole interaction. Points refer to experimental data, lines are numerical solutions to equation (3) at $r = (1)$ 1.18, (2) 1.24, and (3) 1.30 μm. In the inset: the mutual orientation of magnetic dipoles of atoms.

5. Conclusions

Results of the numerical simulation and experimental realisation are presented for the optical pumping of thulium atoms to the central sublevel with $m_F = 0$ of the ground state by using the transition at $\lambda = 530.7$ nm, which also participates in the laser cooling cycle. The optimal values of detunings found experimentally for the pump and repumping radiations $\Delta_1 = -0.1$ MHz, $\Delta_2 = -0.8$ MHz (the numerical simulation yields $\Delta_1 = \Delta_2 = 0$) point to atom heating during optical pumping and to raising pump efficiency in the case of Doppler cooling. According to the modelling data, the pump efficiency can be enhanced by increasing the intensities of the pump and repumping radiations above the values used ($S_1 = 4.4$, $S_2 = 4$). At the parameters mentioned above, the attained population is $\eta = 0.79(2)$, and the atom losses due to heating reach 40%. A scheme is suggested and analysed for the optical pumping at the transition with $\lambda = 418.8$ nm (transition $|J = 7/2\rangle \rightarrow |J' = J = 7/2\rangle$). In this scheme, the atom losses due to heating should be substantially lower. In the near future, we plan studying the optical pumping of thulium atoms by using the developed diode laser system operating at $\lambda = 418.8$ nm.

In addition, the rate of a decrease in the relative population of the sublevel with $m_F = 0$ of the ground state in a magnetic field due to dipole–dipole interaction was measured. The average distance between atoms in an optical lattice found from modelling results is 1.24(6) μm. It is shown that depolarisation at the experimental parameters mentioned imposes no constraints on the interrogation time of the ensemble and on the width of the clock transition resonance.

Acknowledgements. The numerical simulation by A.A. Golovizin, G.A. Vishnyakova, and D.A. Mishin was supported by the Russian Science Foundation (Grant No. 19-12-00137). The experimental part of the work was supported by the Russian Foundation for Basic Research (Grant No. 18-02-00628).

References

1. Ludlow A.D., Boyd M.M., Ye J., Peik E., Schmidt P.O. *Rev. Modern Phys.*, **87** (2), 637 (2015).
2. Lu M., Burdick N.Q., Youn S.H., Lev B.L. *Phys. Rev. Lett.*, **107**, 190401 (2011).
3. Gross C., Bloch I. *Science*, **357** (6355), 995 (2017).
4. Pouliot A., Beica H.C., Carew A., Vorozcovs A., Carlse G., Barrett B., Kumarakrishnan A. *Proc. SPIE*, **10637**, 106370A (2018).
5. Rosenband T., Schmidt P.O., Hume D.B., Itano W.M., Fortier T.M., Stalnaker J.E., Kim K., Diddams S.A., Koelemeij J.C.J., Bergquist J.C., Wineland D.J. *Phys. Rev. Lett.*, **98**, 220801 (2007).
6. Wynands R., Weyers S. *Metrologia*, **S64**, 42 (2005).
7. Campbell G.K., Ludlow A.D., Blatt S., Thomsen J.W., Martin M.J., Miranda M.H.G., Zelevinsky T., Boyd M.M., Ye J., Diddams S.A. *Metrologia*, **45**, 539 (2008).
8. Oelke E., Hutson R.B., Kennedy C.J., Sonderhouse L., Bothwell T., Goban A., Kedar D., Sanner C., Robinson J.M., Marti G.E., Matei D.G., Legero T., Giunta M., Holzwarth R., Riehle F., Sterr U., Ye J. arXiv:1902.02741 [physics.atom-ph] (2019).

9. Sukachev D., Fedorov S., Tolstikhina I., Tregubov D., Kalganova E., Vishnyakova G., Golovizin A., Kolachevsky N., Khabarova K., Sorokin V. *Phys. Rev. A*, **94**, 022512 (2016).
10. Wang Y., Meng Y., Wan J., Yu M., Wang X., Xiao L., Cheng H., Liu L. *Phys. Rev. A*, **97**, 023421 (2018).
11. Micalizio S., Godone A., Levi F., Calosso C. *Phys. Rev. A*, **80**, 023419 (2009).
12. Bhaskar N.D. *Phys. Rev. A*, **47** (6), R4559 (1993).
13. Johansson J.R., Nation P., Nori F. *Comp. Phys. Commun.*, **184**, 1234 (2013).
14. Steck D.A. http://steck.us/teaching (revision 0.12.2, 11 April 2018).
15. Kalganova E., Prudnikov O., Vishnyakova G., Golovizin A., Tregubov D., Sukachev D., Khabarova K., Sorokin V., Kolachevsky N. *Phys. Rev. A*, **96**, 033418 (2017).
16. Kalganova E.S., Golovizin A.A., Shevnin D.Do., Tregubov D.O., Khabarova K.Yu., Sorokin V.N., Kolachevky N.N. *Quantum Electron.*, **48** (5), 415 (2018) [*Kvantovaya Elektron.*, **48** (5), 415 (2018)].
17. Golovizin A., Fedorova E., Tregubov D., Sukachev D., Khabarova K., Sorokin V., Kolachevsky N. arXiv:1809.02215v2 [physics.atom-ph].
18. Cohen-Tannoudji C., Diu B., Laloe F. *Quantum Mechanics* (New York: Wiley, 1977) Vol. 2.